Roarty et al., http://www.jcb.org/cgi/content/full/jcb.201408058/DC1

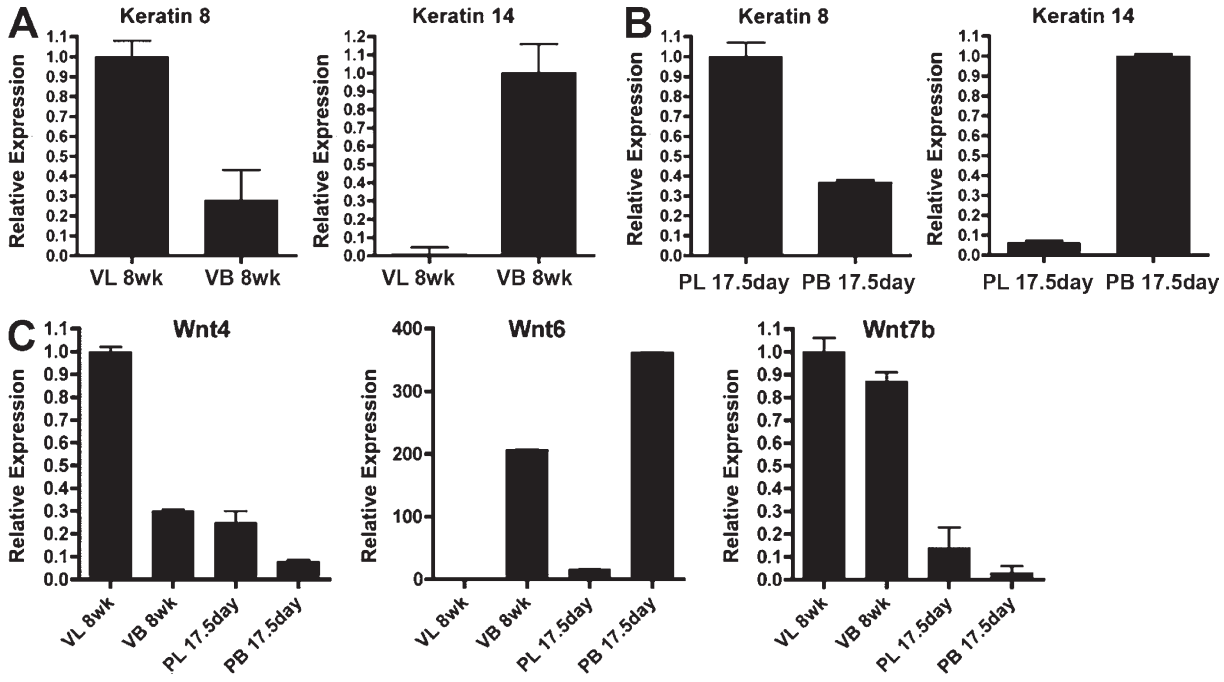

Figure S1. **Sort validation and analysis of additional Wnt ligands in virgin and late pregnant sorted epithelial cells.** (A and B) qRT-PCR analysis of K8 (luminal) and K14 (basal) expression within sorted epithelial fractions from virgin (A) and late pregnant (B) stages of development depicting proper segregation of the populations. (C) qPCR analysis of Wnt4, Wnt6, and Wnt7b within the epithelial fractions among virgin and pregnant stages. VL, virgin luminal; VB, virgin basal; PL, pregnant luminal; PB, pregnant basal. Plotted values represent means ± SD (error bars).

THE JOURNAL OF CELL BIOLOGY

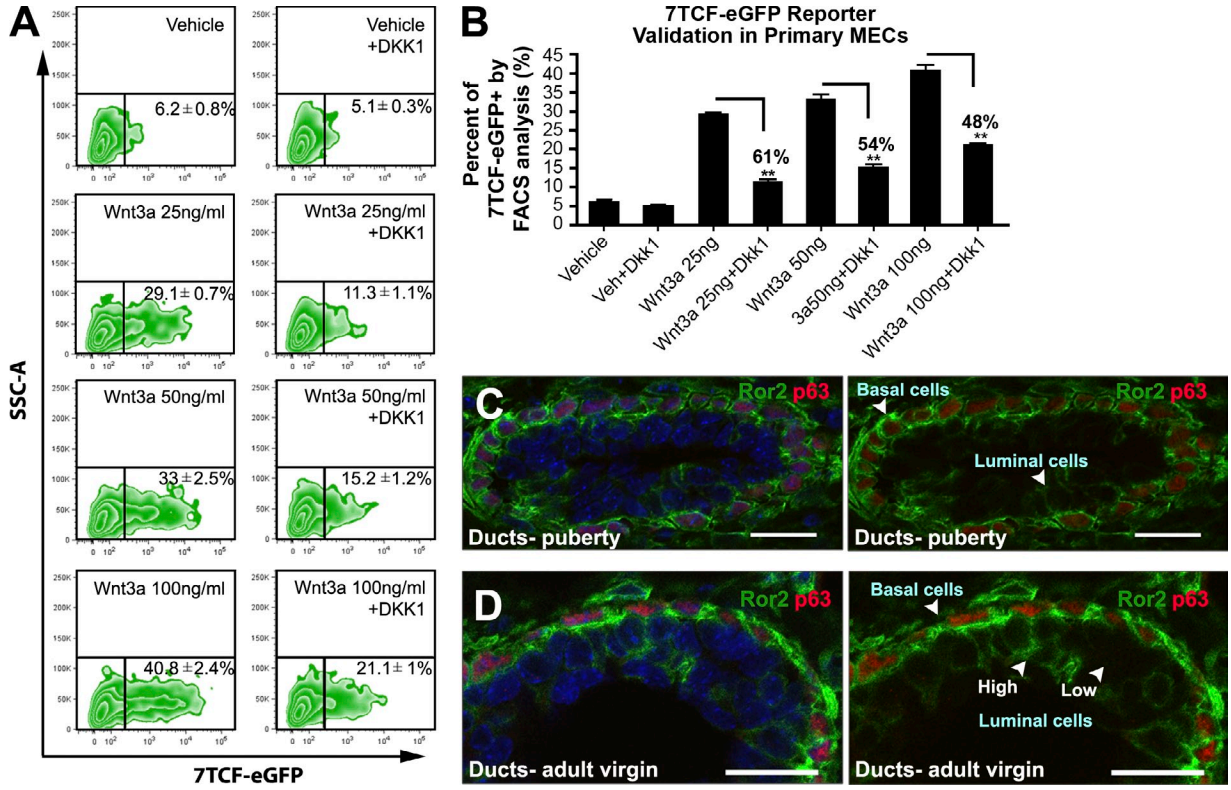

Figure S2. **Validation of the 7TCF-*eGFP* reporter in primary MECs and Ror2 localization in vivo.** (A) FACS plots depicting the induction of 7TCF-*eGFP* activity in response to increasing doses of Wnt3a (left). Plots to the right illustrate the inhibition of reporter activity (7TCF-eGFP) in response to administration of 100 ng/ml DKK1 for each dose of Wnt3a. Shown are representative FACS plots of three experiments, where treatments were performed in triplicate. (B) Quantification of the FACS data in A, depicting the responsiveness of the reporter to Wnt stimulation and inhibition. Percent inhibition is shown for DKK1 treatments. Plotted values represent means ± SD (error bars). **, $P < 0.01$. (C) Ror2 IF staining of trailing ducts in a 6-wk outgrowth during puberty. High Ror2 expression (green) is evident in the basal layer (p63+, red), with gradients of luminal cell Ror2 positivity (arrowheads). (D) Ror2 IF staining of ducts in an 8-wk adult virgin outgrowth. High Ror2 expression is evident in the basal layer (p63+, red), with gradients of luminal cell Ror2 positivity (likely reflecting MP, AP, and LP populations; arrowheads). Bars, 20 µm.

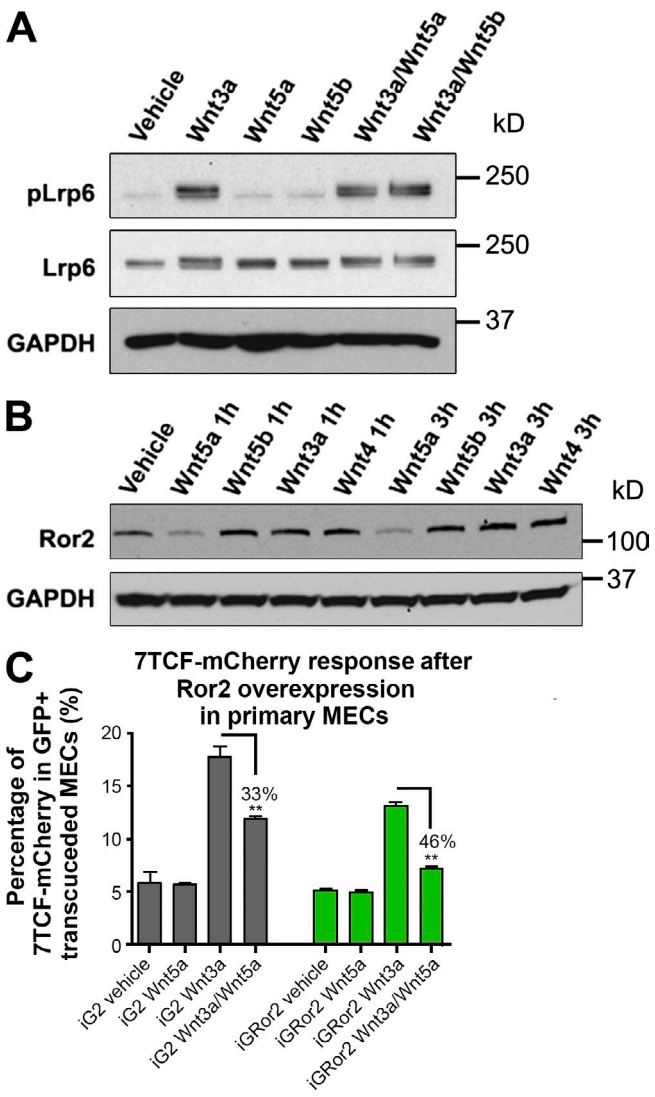

Figure S3. **Treatment of primary MECs with Wnt ligands in vitro.** (A) Western blot for pLRP6 and LRP6 demonstrating the activation of LRP6 by Wnt3a and not Wnt5a or Wnt5b. Levels of pLRP6 are comparable in Wnt3a/Wnt5a and Wnt3a/Wnt5b conditions relative to Wnt3a alone. (B) Western blot for Ror2 protein levels after 1 h and 3 h stimulations with individual Wnt proteins. Ror2 protein is down-regulated after Wnt5a treatment. (C) Plot depicting the FACS-acquired percentages of *7TCF-mCherry* in response to Wnt treatments in iG2 control and iG2-Ror2 overexpressing primary MECs. mCherry expression was analyzed through the eGFP gate, evaluating only transduced cells. Ror2 overexpression enhances the antagonism exhibited by Wnt5a, as was observed with *Axin2* in Fig. 3. Plotted values represent means ± SD (error bars). **, $P < 0.01$.

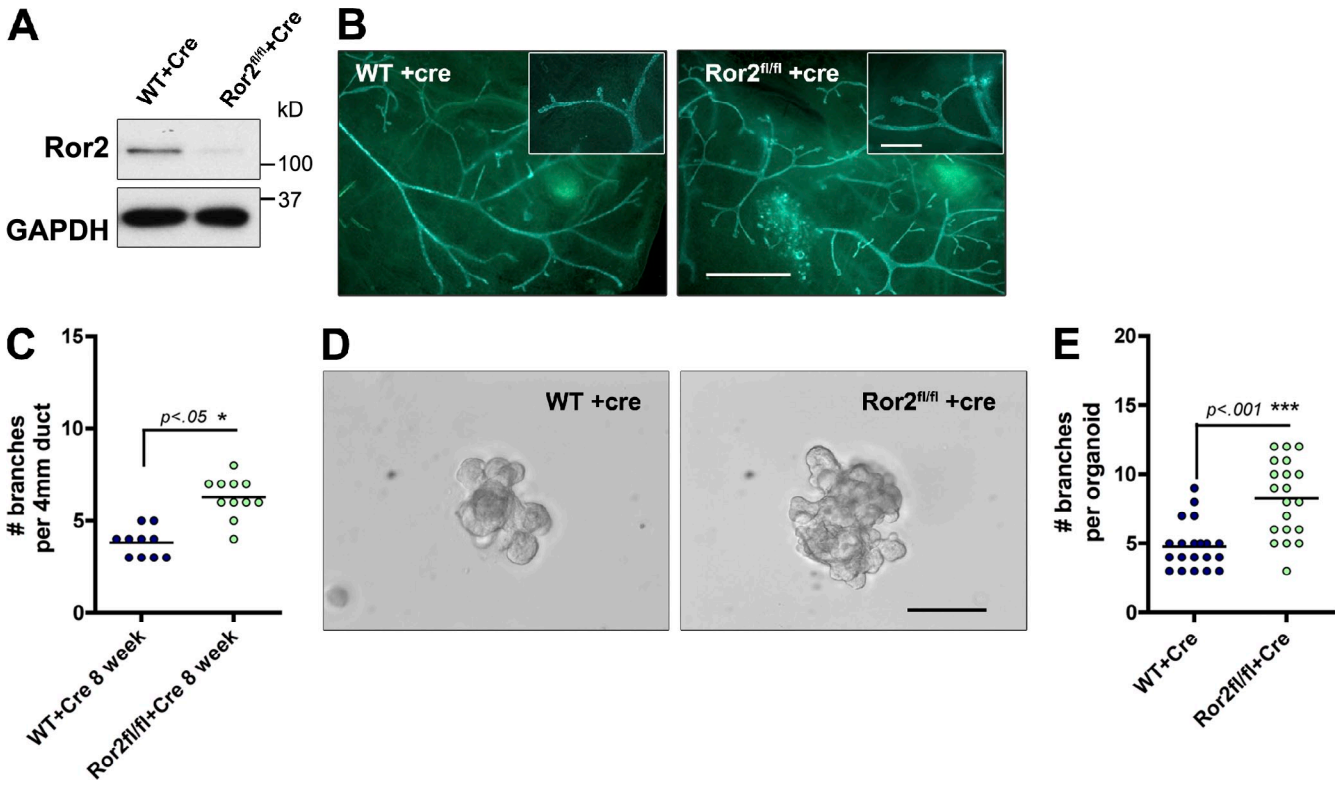

Figure S4. **Lentiviral-Cre deletion of Ror2 recapitulates the branching phenotype exhibited by shRNA depletion in vivo and in vitro.** (A) Western blot for Ror2 in primary MECs after lentiviral-Cre treatment of WT and Ror2$^{fl/fl}$ MECs. (B) Fluorescent whole mounts of contralateral 8-wk outgrowths of lentiviral Cre-treated WT and Ror2$^{fl/fl}$ MECs. Bar, 1.5 mm (inset, 0.5 mm). (C) Quantification of the increase in branching in Ror2$^{fl/fl}$ outgrowths compared with WT outgrowths after lenti-Cre treatment (n = 3 contralateral outgrowths; 3–4 ducts per outgrowth). (D) DIC images of lentiviral Cre-treated WT and Ror2$^{fl/fl}$ organoids after FGF2 administration for 1 wk, demonstrating increased and disorganized branching as a result of Ror2 deletion. Bar, 50 µm. (E) Quantification of the branching exhibited in F between WT +Cre and Ror2$^{fl/fl}$ +Cre groups (n = 20 organoids per group).

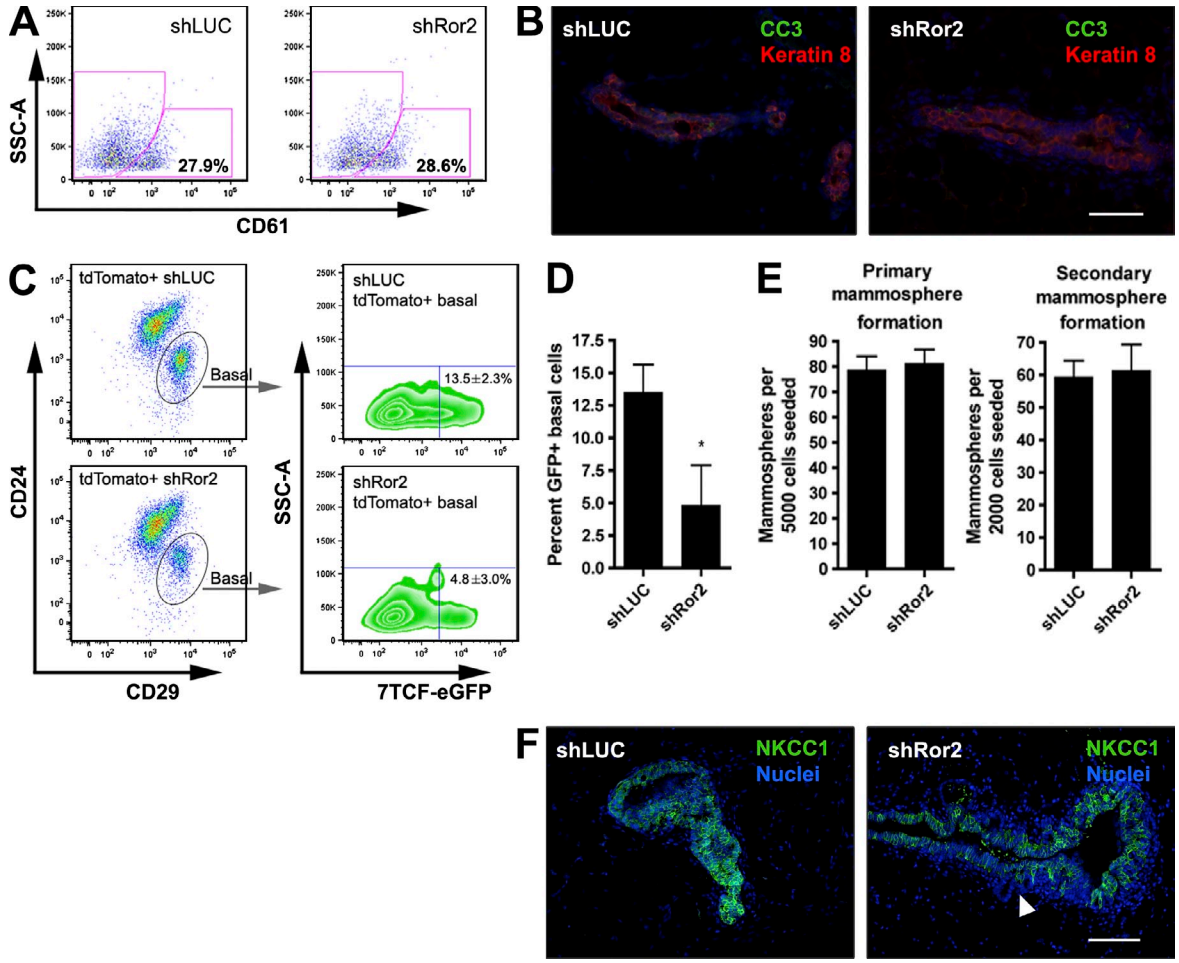

Figure S5. **Phenotypic analysis of shLUC and shRor2 outgrowths.** (A) CD61 FACS analysis of the $CD24^{+}CD29^{lo}$ luminal epithelial fraction depicting equivalent percentages of progenitors within shLUC and shRor2 8-wk outgrowths. Results are representative of $n = 4$ shLUC and shRor2 contralateral groups. (B) IF for cleaved caspase-3 together with K8, illustrating equivalent levels of apoptosis in the ducts of shLUC and shRor2 glands (representative of $n = 5$ mice per group; 4-wk outgrowths). (C) FACS plots depicting the analysis scheme of the basal epithelial fraction from shLUC versus shRor2 8-wk outgrowths co-transduced with the 7TCF-eGFP Wnt reporter. The luminal and basal fractions illustrated are gated based on tdTomato for the presence of the shRNA. The extent of eGFP+ cells within shLUC and shRor2 basal fractions is illustrated. (D) Quantification of eGFP positivity depicting the 2.8-fold decrease in GFP+ cells within shRor2 outgrowths ($n = 3$ pooled outgrowths per group; *, $P < 0.05$). (E) Equivalent primary and secondary mammosphere forming efficiencies between shLUC and shRor2 groups derived from sorted $CD24^{+}CD29^{hi}$ basal fractions of 8-wk outgrowths. Plotted values represent means ± SD (error bars). (F) IF for NKCC1 (green) within the TEB of shLUC and shRor2 4-wk outgrowths. The arrowhead denotes the area of NKCC1 loss around the budding shRor2 TEB neck (representative of $n = 5$ mice per group). Bars, 100 µm.

Table S1. **qRT-PCR primer sequences**

Target	Forward primer (5′–3′)	Reverse primer (5′–3′)
Wnt4	CTGGACTCCCTCCCTGTCTT	ATGCCCTTGTCACTGCAAA
Wnt5a	ACGCTTCGCTTGAATTCCT	CCCGGGCTTAATATTCCAA
Wnt5b	GAGAGCGTGAGAAGAACTTTGC	GGCGACATCAGCCATCTTAT
Wnt6	GTGCAACTGCACAACAACG	GGAACGGAGGCAGCTTCT
Wnt7b	TCATGAACCTTCACAACAATGA	TGGTCCAGCAAGTTTTGGT
Ror1	TCAATGCATACAAGCCCAAG	TTCTTCCATGAAACGCACAG
Ror2	TCATCAGCCAGCACAAACA	GTGGCCTTTGTAGACCTTGC
Axin2	GAGAGTGAGCGGCAGAGC	CGGCTGACTCGTTCTCCT
Cytokeratin 8	AGTTCGCCTCCTTCATTGAC	GCTGCAACAGGCTCCACT
Cytokeratin 14	ATCGAGGACCTGAAGAGCAA	TCGATCTGCAGGAGGACATT
Actin	GCAACGAGCGGTTCCG	CCCAAGAAGGAAGGCTGGA

Forward and reverse primer sequences are listed for the targets *Wnt4*, *Wnt5a*, *Wnt5b*, *Wnt6*, *Wnt7b*, *Ror1*, *Ror2*, *Axin2*, *Cytokeratin8*, *Cytokeratin14*, and *Actin*.